# New Types of Solutions of Non-Linear Fractional Differential Equations

Mark Edelman and Laura Anna Taieb

**Abstract.** Using the Riemann-Liouville and Caputo Fractional Standard Maps (FSM) and the Fractional Dissipative Standard Map (FDSM) as examples, we investigate types of solutions of non-linear fractional differential equations. They include periodic sinks, attracting slow diverging trajectories (ASDT), attracting accelerator mode trajectories (AMT), chaotic attractors, and cascade of bifurcations type trajectories (CBTT). New features discovered include attractors which overlap, trajectories which intersect, and CBTTs.

**Mathematics Subject Classification (2000).** Primary 47Gxx; Secondary 47Hxx.

**Keywords.** Discrete map, attractor, fractional dynamical system, map with memory, stability.

## 1. Introduction

In recent years fractional calculus (FC) and fractional differential equations (FDE) became very popular in many areas of science. The books dedicated to the applications of FDEs published in 2010-2011 include [1, 2, 3] in physics in general, [4, 5] in modeling and control, [6] in viscoelasticity, [7] in systems with long-range interaction. A good review of applications of FC to chaos in Hamiltonian Systems is given in [8]. Because fractional derivatives are integro-differential operators, they are used to describe systems distributed in time and/or space: systems with long range interaction [7, 9, 10, 11, 12, 13], non-Markovian systems with memory ([14] Ch.10, [15, 16, 17, 18, 19]), fractal media [20], etc. Biological systems are probably the best examples of systems with memory. As it has been shown recently [21, 22], even processing of external stimuli by individual neurons can be described by fractional differentiation. In some cases [23, 24, 25, 26] FDEs are equivalent to the Volterra integral equations of the second kind. This kind of equations (non

This work was completed with the support of Yeshiva University, Courant Institute of Mathematical Sciences, and DOE Grant DE-FG0286ER53223.

necessarily FDEs) is used in nonlinear viscoelasticity (see for example [27, 28]) and in biology (for applications to mathematical models in population biology and epidemiology see [29, 30]).

As in regular dynamics (in application to various areas in science), the nonlinearity plays a significant role in fractional dynamics. Chaos and order in nonlinear systems with long range interactions were considered in [7, 10, 11, 12], nonlinear FDEs in application to the control were reviewed in books [4, 5], nonlinear fractional reaction-diffusion systems considered in [31, 32, 33, 34]. Corresponding to the fact that in physical systems the transition from integer order time derivatives to fractional (of a lesser order) introduces additional damping similar in appearance to additional friction [14, 35], phase spaces of the systems with fractional time derivatives demonstrate different kinds of structures similar to the attractors of the dissipative dynamical systems [4, 35, 36].

As in the case of the systems which can be described by regular differential equations, general properties of systems described by FDEs can be demonstrated on the examples of maps which can be derived by integrating the FDEs (if it is possible) over a period of perturbation. Equations of some fractional maps (FM), which include among others fractional standard maps (FSM) and fractional dissipative standard maps (FDSM), were derived in a series of recent publications [7, 37, 38, 39, 40, 26] from the corresponding FDEs.

Two of the most studied examples in the regular case are the Chirikov standard map (SM) [41] and the Zaslavsky dissipative standard map (DSM) [42, 43]. The SM provides the simplest model of the universal generic area preserving map and the description of many physical systems and effects (Fermi acceleration, comet dynamics, etc.) can be reduced to the studying of the SM. The topics examined include fixed points, elementary structures of islands and a chaotic sea, and fractional kinetics [41, 44, 45]. Different properties of the DSM were discussed in [46, 47, 48, 49, 50, 51], and a rigorous proof of the existence of chaotic attractor in such type of systems was obtained in [52, 53]. It was also proved in [52, 53] that the system of this type exhibits quasi-periodic attractors, periodic sinks, transient chaos with the dynamics attracting to the sink, and the existence of the SRB measure for the purely chaotic dynamics. All this stimulated the study of the FSMs [38, 54] and FDSM [39] in hope to reveal the most general properties of the fractional dynamics.

Two-dimensional maps investigated in [38, 39, 54] were derived from the FDEs (see Section 2) and, as a result, they are discrete maps with memory in which the present state of evolution depends on all past states. The earlier studies of maps with memory were done on one-dimensional maps which were not derived from differential equations [55, 56, 57, 58, 59, 60]. Most results were obtained for the generalizations of the logistic map and the main general result is that the presence of memory makes systems more stable. The initial study of the FSM in [38, 39, 54] was concentrated on the investigation of the fixed/periodic points' stability of the FSM, new properties and new types of attractors.

The results obtained in [38, 39, 54] revealed new unusual properties of the fractional attractors of the FSM, which are different not only from the properties of the fixed/periodic points of the non-dissipative systems (the SM in our case), but also from the properties of attractors of the regular (not fractional) dissipative systems (e.g. the DSM). The most unusual observed property of the FSMs is the existence (and persistence) of the new type of attractors - cascade of bifurcations type trajectories (CBTT). A cascade of bifurcations, when with the change in the value of a parameter a system undergoes a sequence of period-doubling bifurcations, is a well known pathway of a transition form order to chaos. In the case of the CBTT the period doubling occurs without a change in a system parameter and is an internal property of a system. In Section 3 we summarize results of the extensive numerical investigation of three fractional maps to demonstrate the properties of fractional attractors. An analysis of the conditions for the CBTTs' appearance will be presented in the following publications.

## 2. Basic Equations

The standard map in the form

$$p_{n+1} = p_n - K \sin x_n, \quad x_{n+1} = x_n + p_{n+1} \pmod{2\pi} \tag{2.1}$$

can be derived from the differential equation

$$\ddot{x} + K \sin(x) \sum_{n=0}^{\infty} \delta\Big(\frac{t}{T} - (n+\varepsilon)\Big) = 0, \tag{2.2}$$

where $\varepsilon \to 0+$, following the steps proposed by Tarasov in [26].

The equations for the Riemann-Liouville FSM (FSMRL) were obtained in [37] and [26]. Following the steps proposed [26], the FSMRL in the form which converges to the SM as $\alpha \to 2$ can be derived from the differential equation with the Riemann-Liouville fractional derivative describing a kicked system

$${}_0D_t^{\alpha} x + K \sin(x) \sum_{n=0}^{\infty} \delta\Big(\frac{t}{T} - (n+\varepsilon)\Big) = 0, \quad (1 < \alpha \le 2), \tag{2.3}$$

where $\varepsilon \to 0+$, with the initial conditions

$$({}_0D_t^{\alpha-1} x)(0+) = p_1, \quad ({}_0D_t^{\alpha-2} x)(0+) = b, \tag{2.4}$$

where

$${}_0D_t^{\alpha} x(t) = D_t^n \, {}_0I_t^{n-\alpha} x(t) =$$

$$\frac{1}{\Gamma(n-\alpha)} \frac{d^n}{dt^n} \int_0^t \frac{x(\tau) d\tau}{(t-\tau)^{\alpha-n+1}} \quad (n-1 < \alpha \le n), \tag{2.5}$$

$D_t^n = d^n/dt^n$, and ${}_0I_t^{\alpha}$ is a fractional integral.

After integration of equation (2.3) the FSMRL can be written in the form

$$p_{n+1} = p_n - K \sin x_n, \tag{2.6}$$

$$x_{n+1} = \frac{1}{\Gamma(\alpha)} \sum_{i=0}^{n} p_{i+1} V_\alpha^1(n-i+1), \quad (\mathrm{mod}\ 2\pi), \tag{2.7}$$

where

$$V_\alpha^k(m) = m^{\alpha-k} - (m-1)^{\alpha-k} \tag{2.8}$$

and momentum $p(t)$ is defined as

$$p(t) = {}_0D_t^{\alpha-1} x(t). \tag{2.9}$$

Here it is assumed that $T = 1$ and $1 < \alpha \leq 2$. The condition $b = 0$ is required in order to have solutions bounded at $t = 0$ for $\alpha < 2$ [38]. In this form the FSMRL equations in the limiting case $\alpha = 2$ coincide with the equations for the standard map under the condition $x_0 = 0$. For consistency and in order to compare corresponding results for all three maps (the SM, the FSMRL, and the Caputo FSM (FSMC)) all trajectories considered in this article have the initial condition $x_0 = 0$.

Following the steps proposed [26], the FSMC in the form which converges to the SM as $\alpha \to 2$ can be derived from the differential equation similar to (2.3) but with the Caputo fractional derivative

$${}_0^C D_t^\alpha x + K \sin(x) \sum_{n=0}^{\infty} \delta\Big(\frac{t}{T} - (n+\varepsilon)\Big) = 0, \quad (1 < \alpha \leq 2) \tag{2.10}$$

where $\varepsilon \to 0+$, with the initial conditions

$$p(0) = ({}_0^C D_t^1 x)(0) = (D_t^1 x)(0) = p_0, \quad x(0) = x_0, \tag{2.11}$$

where

$${}_0^C D_t^\alpha x(t) = {}_0\, I_t^{n-\alpha}\ D_t^n x(t) =$$
$$\frac{1}{\Gamma(n-\alpha)} \int_0^t \frac{D_\tau^n x(\tau) d\tau}{(t-\tau)^{\alpha-n+1}} \quad (n-1 < \alpha \leq n). \tag{2.12}$$

Integrating equation (2.10) with the momentum defined as $p = \dot{x}$ and assuming $T = 1$ and $1 < \alpha \leq 2$, one can derive the FSMC in the form

$$p_{n+1} = p_n - \frac{K}{\Gamma(\alpha-1)} \Big[ \sum_{i=0}^{n-1} V_\alpha^2(n-i+1) \sin x_i + \sin x_n \Big], \quad (\mathrm{mod}\ 2\pi), \tag{2.13}$$

$$x_{n+1} = x_n + p_0 - \frac{K}{\Gamma(\alpha)} \sum_{i=0}^{n} V_\alpha^1(n-i+1) \sin x_i, \quad (\mathrm{mod}\ 2\pi). \tag{2.14}$$

It is important to note that the FSMC ((2.13), (2.14)) can be considered on a torus ($x$ and $p$ mod $2\pi$), a cylinder ($x$ mod $2\pi$), or in an unbounded phase space, whereas the FSMRL ((2.6), (2.7)) can be considered only in a cylindrical or an unbounded phase space. The FSMRL has no periodicity in $p$ and cannot be considered on a torus. This fact is related to the definition of momentum (2.9) and initial conditions

(2.4). The comparison of the phase portraits of two FSMs is still possible if we compare the values of the $x$ coordinates on the trajectories corresponding to the same values of the maps' parameters.

The DSM in the form

$$X_{n+1} = X_n + P_{n+1}, \tag{2.15}$$

$$P_{n+1} = -bP_n - Z\,\sin(X_n) \tag{2.16}$$

can be derived integrating the differential equation of the the kicked damped rotator (see for example [39])

$$\ddot{X} + q\dot{X} = \varepsilon \sin(X) \sum_{n=0}^{\infty} \delta\Big(t - n\Big). \tag{2.17}$$

Two forms of the FDSM were derived in [7, 37, 39]. The form which has been investigated numerically in [39]

$$X_{n+1} = \frac{\mu^{-1}}{\Gamma(\alpha-1)} \sum_{k=0}^{n} P_{k+1} W_\alpha(q, k-n-1), \tag{2.18}$$

$$P_{n+1} = -bP_n - Z \sin(X_n), \tag{2.19}$$

where functions $W_\alpha(a,b)$ are defined by

$$W_\alpha(a,b) = a^{1-\alpha} e^{a(b+1)} \Big[\Gamma(\alpha-1, ab) - \Gamma(\alpha-1, a(b+1))\Big] \tag{2.20}$$

and $\Gamma(a,b)$ is the incomplete Gamma function

$$\Gamma(a,b) = \int_b^\infty y^{a-1} e^{-y} dy \tag{2.21}$$

has been derived from the following fractional generalization of (2.17)

$${}_0D_t^\alpha X(t) - q\,{}_0D_t^\beta X(t) = \varepsilon \sin(X) \sum_{n=0}^{\infty} \delta(t-n), \tag{2.22}$$

where

$$q \in \mathbb{R}, \quad 1 < \alpha \le 2, \quad \beta = \alpha - 1.$$

Here

$$\mu = (1 - e^{-q})/q, \quad Z = -\mu\varepsilon e^q. \tag{2.23}$$

Further in this paper we will also use $K = \varepsilon \exp(q)$ and $\Gamma = -q$.

## 3. Fractional Attractors

### 3.1. Standard Map: Fixed and Periodic Points

It appears that the dependence of the SM's fixed point (0,0) stability properties on the map parameter $K$ plays an important role when transition to the FSMs is considered. (0,0) SM fixed point is stable for $0 < K < 4$. At $K = 4$ it becomes unstable but period two ($T = 2$) antisymmetric trajectory

$$p_{n+1} = -p_n, \quad x_{n+1} = -x_n \tag{3.1}$$

appears which is stable for $4 < K < 2\pi$. At $K = 2\pi$ this T=2 trajectory becomes unstable but it gives birth to two $T = 2$ trajectories [41, 44] with

$$p_{n+1} = -p_n, \quad x_{n+1} = x_n - \pi. \tag{3.2}$$

These $T = 2$ trajectories become unstable when $K \approx 6.59$ (see Figure 4a), at the point where $T = 4$ stable trajectories are born. This period doubling cascade of bifurcations sequence continues with $T = 8$ and $T = 16$ stable trajectories appearing at $K \approx 6.63$ and $K \approx 6.6344$ correspondingly. It continues until at $K \approx 6.6345$ all periodic points become unstable and corresponding islands disappear. This scenario of the elliptic-hyperbolic point transitions with the births of the double periodicity islands inside the original island has been investigated in [61] and applied to investigate the SM stochasticity at low values of the parameter $K < 4$.

### 3.2. Phase Space at Low $K$ (Stable (0,0) Fixed Point)

Stability of the fixed point (0,0) has been considered in [38, 54]. It has been shown that for fractional values of $\alpha$ (we consider only $1 < \alpha \leq 2$) this point turns from elliptic (for $\alpha = 2$) into a sink which is stable for

$$K < K_{c1}(\alpha) = \frac{2\Gamma(\alpha)}{V_{\alpha l}}, \tag{3.3}$$

where

$$V_{\alpha l} = \sum_{k=1}^{\infty} (-1)^{k+1} V_{\alpha}^{1}(k) \tag{3.4}$$

and can be calculated numerically (see Figure 4a). It can be shown that $K_{c1}(2) = 4$, which corresponds to the SM case. The structure of the FSM phase space for $K < K_{c1}$ preserves some features which exist in the $\alpha = 2$ case. Namely, stable higher period points, which exist in the SM case, still exist in the FSM, but they exist in the asymptotic sense and they transform into sinks or, in the FSMRL case, into attracting slow ($p_n \sim n^{2-\alpha}$) diverging trajectories (ASDT) (see Figure 1). Pure chaotic trajectories disappear. Each attractor has its own basin of attraction. The traces of the SM chaotic sea exist in the following sense: initially close trajectories, which do not start from any basin of attraction, may fall into absolutely different attractors. In most of the cases attracting points themselves do not belong to their own basins of attraction: trajectory which starts from an attracting point may fall into a different attractor. The FSMRL trajectories which converge to

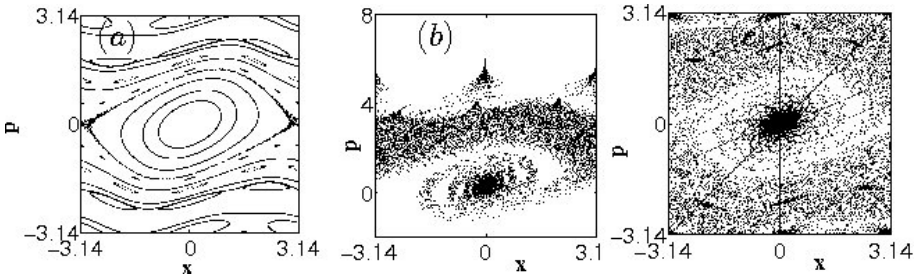


FIGURE 1. (a). 1000 iterations on each of 25 trajectories for the SM with $K = 0.6$. The main features are (0,0) fixed point and T=2 and T=3 trajectories; (b). 400 iterations on each trajectory with $p_0 = 2 + 0.04i$, $0 \leq i < 50$ for the FSMRL case $K = 0.6$, $\alpha = 1.9$. Trajectories converging to the fixed point and ASDTs of period 2 and 3 are present; (c). 100 iterations on each FSMC trajectory with $p_0 = -3.14 + 0.0314i$, $0 \leq i < 200$ for the same case as in Fig. 1b ($K = 0.6$, $\alpha = 1.9$) considered on a torus. In this case all trajectories converge to the fixed point, period two and period three stable attracting points.

the fixed point follow two different routs. Trajectories which start from the basin of attraction converge according to the power law $x_n \sim n^{-1-\alpha}$ and $p_n \sim n^{-\alpha}$, while those starting from the outside of the basin of attraction are attracting slow converging trajectories (ASCT) with $x_n \sim n^{-\alpha}$ and $p_n \sim n^{1-\alpha}$. All FSMC trajectories converging to $(0, 0)$ fixed point follow the slow power law $x_n \sim n^{1-\alpha}$ and $p_n \sim n^{1-\alpha}$ (see Figure 2). This convergence may correspond to the recently introduced for the fractional dynamic systems notion of the generalized Mittag-Leffler stability [62], for which the power-law stability is a special case.

### 3.3. Phase Space at $K_{c1} < K < K_{c2}$ (Stable $T = 2$ Antisymmetric Trajectory)

Numerical simulations confirm that, as in the SM case, in the FSMs a period $T = 2$ antisymmetric trajectory (sink) exists (asymptotically) for $K_1(\alpha) < K < K_2(\alpha)$ ($4 < K < 2\pi$ in the SM case) with

$$p_{n+1} = -p_n, \quad x_{n+1} = -x_n. \tag{3.5}$$

Asymptotic existence and stability of this sink is a result of the gradual transformation of the SM's elliptic point with the decrease in the order of derivative from $\alpha = 2$ (see Figure 3). As in the fixed point case, there are two types of convergence of the trajectories to the FSMRL $T = 2$ sink: fast with

$$\delta x_n \sim n^{-1-\alpha}, \quad \delta p_n \sim n^{-\alpha} \tag{3.6}$$

and slow with

$$\delta x_n \sim n^{-\alpha}, \quad \delta p_n; \sim n^{1-\alpha} \tag{3.7}$$

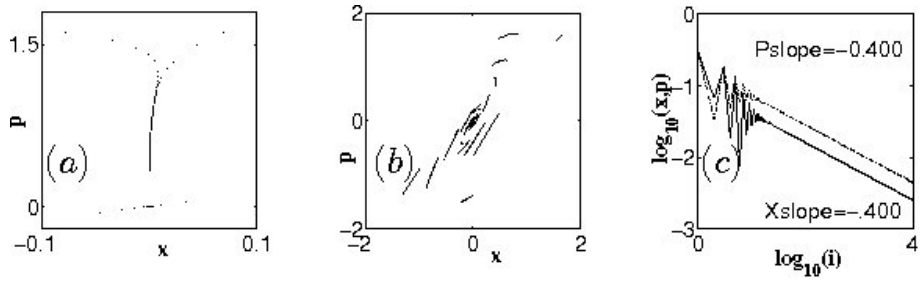


FIGURE 2. Convergence of trajectories to the fixed point $(0, 0)$ at $K < K_{c1}$: (a). Two trajectories for the FSMRL with $K = 2$, $\alpha = 1.4$, and $10^5$ iterations on each trajectory. The bottom one with $p_0 = 0.3$ is a fast converging trajectory. The upper trajectory with $p_0 = 5.3$ is an example of the FSMRL's ASCT; b). Evolution of the FSMC trajectories with $p_0 = 1.6 + 0.002i$, $0 \le i < 50$ for the case $K = 3$, $\alpha = 1.9$. The line segments correspond to the $n$th iteration on the set of trajectories with close initial conditions; c). $x$ and $p$ time dependence for the FSMC with $K = 2$, $\alpha = 1.4$, $x_0 = 0$, and $p_0 = 0.3$.

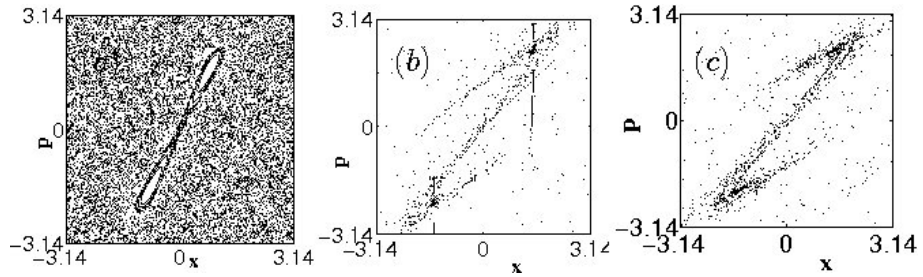


FIGURE 3. Stable antisymmetric $x_{n+1} = -x_n$, $p_{n+1} = -p_n$ period $T = 2$ trajectories for $K = 4.5$: (a). 1000 iterations on each of 25 trajectories for the SM with $K = 4.5$. The only feature is a system of two islands associated with the period two elliptic point; (b). The FSMRL stable $T = 2$ antisymmetric sink for $\alpha = 1.8$. 500 iterations on each of 25 trajectories: $p_0 = 0.0001 + 0.08i$, $0 \le i < 25$. Slow and fast converging trajectories; (c). The FSMC stable $T = 2$ antisymmetric sink for $\alpha = 1.8$. 1000 iterations on each of 10 trajectories: $p_0 = -3.1415 + 0.628i$, $0 \le i < 10$.

and

$$\delta x_n \sim n^{1-\alpha}, \quad \delta p_n \sim n^{1-\alpha} \tag{3.8}$$

convergence in the FSMC case [54].

Let's consider the FSMRL and assume the asymptotic existence of the $T = 2$ sink $(x_l, p_l)$ and $(-x_l, -p_l)$. In this case the limit $n \to \infty$ in (2.6) and (2.7) gives

$$p_l = \frac{K}{2}\sin(x_l), \tag{3.9}$$

$$x_l = \frac{K}{2\Gamma(\alpha)}\sin(x_l)\sum_{k=1}^{\infty}(-1)^{k+1}V_\alpha^1(k). \tag{3.10}$$

The equation for $x_l$ takes the form

$$x_l = \frac{K}{2\Gamma(\alpha)}V_{\alpha l}\sin(x_l), \tag{3.11}$$

from which the condition of the existence of the $T = 2$ sink is

$$K > K_{c1}(\alpha) = \frac{2\Gamma(\alpha)}{V_{\alpha l}}. \tag{3.12}$$

From (3.12) it follows that $K_1(\alpha) = K_{c1}(\alpha)$.

- **Remark 1:** The $T = 2$ sink exists only in the asymptotic sense. On a trajectory which starts from point $(x_0, p_0)$=$(x_l, p_l)$ $x_2 \neq x_l$ and $p_2 \neq p_l$.
- **Remark 2:** In spite of the fact that in the derivation of (3.9) and (3.10) we used the limit $n \to \infty$, computer simulations demonstrate convergence of all trajectories to the limiting values in the very good agreement with (3.6), (3.7), and (3.8).
- **Remark 3:** Direct computations show that $K_1(\alpha) = K_{c1}(\alpha)$ is valid for the FSMC too.

### 3.4. Phase Space at $K > K_{c2}$

The SM's $T = 2$ antisymmetric trajectory becomes unstable when $K = 2\pi$, at the point in phase space where a pair of $T = 2$ trajectories with $x_{n+1} = x_n - \pi$, $p_{n+1} = -p_n$ appears. Numerical simulations show (see Figure 5) that the FSMs demonstrate similar behavior. Let's assume that the FSMRL equations (2.6) and (2.7) have an asymptotic solution

$$p_n = (-1)^n p_l, \quad x_n = x_l - \frac{\pi}{2}[1 - (-1)^n]. \tag{3.13}$$

Then it follows from (2.6) that relationship (3.9) $p_l = K/2\sin(x_l)$ holds in this case too. Simulations similar to those presented in Figure 2b [63] show that for $K > K_{c2}$ (see Figure 4a) the FSMRL has an asymptotic solution

$$p_n = (-1)^n p_l + An^{1-\alpha} \tag{3.14}$$

with the same $A$ for both even and odd values of $n$. Substituting (3.14) in (2.7) and considering limit $n \to \infty$ one can derive (see [63])

$$\sin(x_l) = \frac{\pi\Gamma(\alpha)}{KV_{\alpha l}}, \tag{3.15}$$

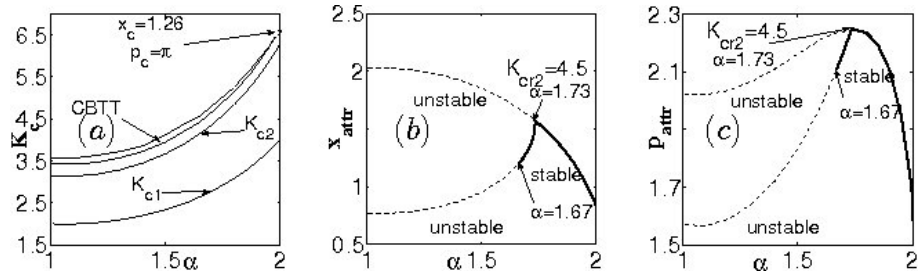


FIGURE 4. Critical values in the FSMs' $(\alpha, K)$-space. The results obtained by the numerical simulations of equations (3.12), (3.16), (3.11), (3.15), (3.9) and confirmed by the direct simulations of the FSMs: (a). The $(0, 0)$ fixed point is stable below $K = K_{c1}$ curve. It becomes unstable at $K = K_{c1}$ and gives birth to the antisymmetric $T = 2$ sink which is stable at $K_{c1} < K < K_{c2}$. A pair of $T = 2$ sinks with $x_{n+1} = x_n - \pi$, $p_{n+1} = -p_n$ is stable in the band above $K = K_{c2}$ curve. Cascade of bifurcations type trajectories (CBTTs) are the only phase space features that appear and exist in the narrow band which ends at the cusp on the figure. $(x_c, p_c)$ is the point at which the SM's $T = 2$ elliptic points with $x_{n+1} = x_n - \pi$, $p_{n+1} = -p_n$ become unstable and bifurcate (see Sec. 3.1); (b). $\alpha$-dependence of the $T = 2$ sinks' x-coordinate for $K = 4.5$. The transition from the antisymmetric sink (upper curve) to $x_{n+1} = x_n - \pi$, $p_{n+1} = -p_n$ point takes place at $\alpha = 1.73$. Solid lines represent areas of stability; (c). $K = 4.5$ $\alpha$-dependence of the $T = 2$ sinks' p-coordinate.

which has solutions for

$$K > K_{c2} = \frac{\pi\Gamma(\alpha)}{V_{\alpha l}} \tag{3.16}$$

(see Figure 4) and the value of $A$ can also be calculated:

$$A = \frac{2x_l - \pi}{2\Gamma(2-\alpha)}. \tag{3.17}$$

These results are in a good agreement with the direct FSMRL numerical simulations and hold for the FSMC.

### 3.5. Cascade of Bifurcations Type Trajectories

In the SM further increase in $K$ at $K \approx 6.59$ causes an elliptic-hyperbolic point transition when $T = 2$ points become unstable and stable $T = 4$ elliptic points appear. A period doubling cascade of bifurcations leads to the disappearance of the corresponding islands of stability in the chaotic sea at $K \approx 6.6344$. The cusp in Figure 4a points to approximately this spot ($\alpha = 2$, $K \approx 6.63$). Inside of the band leading to the cusp a new type of the FSM's attractors appears: cascade of

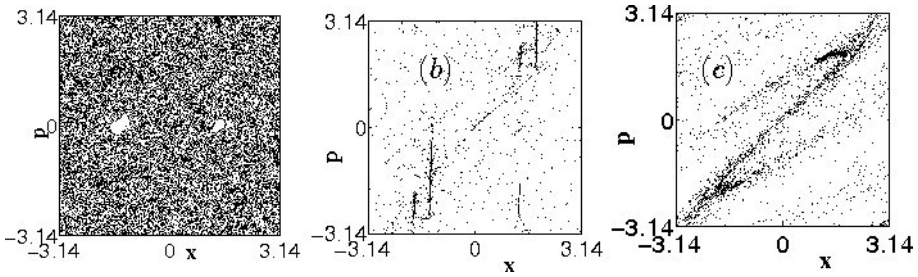


FIGURE 5. Stable $x_{n+1} = x_n - \pi$, $p_{n+1} = -p_n$ period $T = 2$ trajectories for $K > K_{c2}$: (a). 500 iterations on each of 50 trajectories for the SM with $K = 6.4$. The main features are two accelerator mode sticky islands around points $(-1.379, 0)$ and $(1.379, 0)$ which define the dynamics. Additional features - dark spots at the top and the bottom of the figure (which are clear on a zoom) - two systems of $T = 2$ tiny islands associated with two $T = 2$ elliptic points: $(1.379, \pi)$, $(1.379 - \pi, -\pi)$ and $(\pi - 1.379, \pi)$, $(-1.379, -\pi)$; (b). Two FSMRL's stable $T = 2$ sinks for $K = 4.5$, $\alpha = 1.71$. 500 iterations on each of 25 trajectories: $p_0 = 0.0001 + 0.08i$, $0 \le i < 25$; (c). Two FSMC's stable $T = 2$ sinks for $K = 4.5$, $\alpha = 1.71$. 1000 iterations on each of 10 trajectories: $p_0 = -3.1415 + 0.628i$, $0 \le i < 10$.

bifurcations type trajectories (CBTT) (see Figure 6). In CBTTs period doubling cascade of bifurcations occurs on a single trajectory without any change in the map parameter. In some cases CBTTs behave like sticky islands of the Hamiltonian dynamics: occasionally a trajectory enters a CBTT and then leaves it entering the chaotic sea. Near the cusp CBTTs are barely distinguishable - the relative time trajectories spend in CBTTs is small. With decrease in $\alpha$ the relative time trajectories spend in CBTTs increases and at $\alpha$ close to one a trajectory enters a CBTT after a few iterations and stays there over the longest computational time we were able to run our codes - 500000 iterations. A typical FSMC's CBTT of this kind is presented in the Figure 7c.

CBTTs, easily recognizable in the phase space of the FSMRL (Figure 6a), often almost impossible to distinguish in the phase space of the FSMC (Figure 6b). But they clearly reveal themselves on a coordinate versus time (step of iteration $n$) plot (Figure 6c).

### 3.6. More FSM's attractors

The main feature of the SM's phase space at $K > 2\pi$, which defines dynamics and transport and is well investigated (see for example [64]), is the presence of the sticky accelerator mode islands. Slight decrease in the order of derivative turns accelerator mode islands into attracting accelerator mode trajectories (AMT) (Figure 7a).

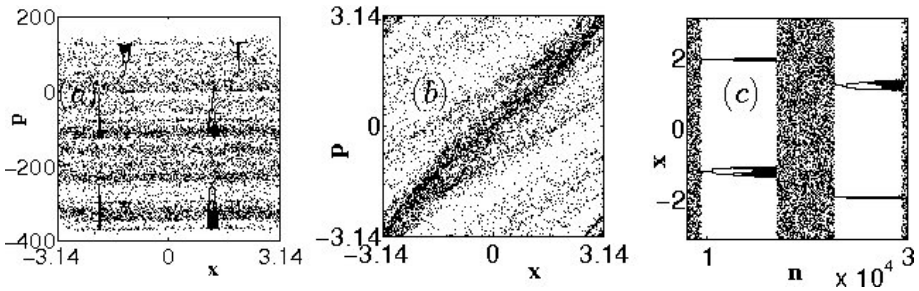


FIGURE 6. Cascade of bifurcations type trajectories (CBTT) from iterations on a single trajectory with $K = 4.5$, $\alpha = 1.65$, $x_0 = 0$, and $p_0 = 0.3$: (a). 25000 iterations for the FSMRL case. The trajectory occasionally sticks to one of the cascade of bifurcations type trajectories but later always returns to the chaotic sea; (b). 30000 iterations for the FSMC case. The CBTTs can hardly be recognized on the full phase portrait but can be seen on the $x$ of $n$ dependence in Figure 6c; (c). Time dependence of the coordinate $x$ in Figure 6b.

Depending on the values of $K$ and $\alpha$ trajectories either permanantly sink into this attractor, or intermittently stick to it and return to the chaotic sea. AMTs do not exist (we were unable to find them) for $\alpha < 1.995$. In the $(\alpha, K)$-plot (Figure 4a) the area of the AMT existence is a part ($K > 2\pi$) of a very narrow strip near $\alpha = 2$ line. In the area of the $\alpha, K$-plot above the CBTT strip (we considered only $K < 7$) different kinds of chaotic attractors (or possibly pure chaotic behavior) can be found. Two examples are presented in Figure 7. Figure 7c contains two overlapping attractors one of which is a CBTT. Existence of the overlapping attractors and intersecting trajectories is a feature of maps with memory which is impossible in a regular dynamical systems. The simplest example of intersecting trajectories can be constructed by starting one trajectory at an arbitrary point $(x_0, p_0)$ and then the second at $(x_0', p_0') = (x_1, p_1)$.

### 3.7. The Fractional Dissipative Standard Map (FDSM)

Consideration of the FDSM in [39] demonstrated that already a small deviation of $\alpha$ from 2 leads to significant changes in properties of the map. For example, a window of ballistic motion which exists in Zaslavsky Map near $K = 4\pi$ is closing when $\alpha < 1.996$. Further decrease in $\alpha$ at $K \approx 4\pi$ produces different kinds of chaotic attractors and sinks [39].

Some of the new features we observed, which are presented in Figure 8, include inverse cascade of bifurcations and trajectories which start as a CBTT and then converge as an inverse cascade of bifurcations. In phase space those trajectories may look like chaotic attractors.

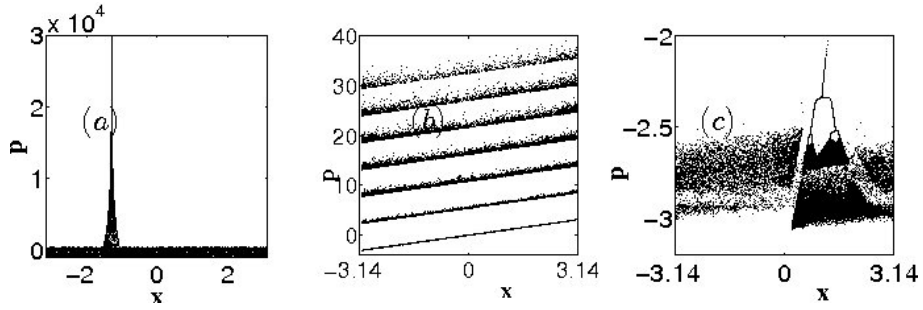


FIGURE 7. (a). A single FSMRL ballistic trajectory for $K = 1.999$, $\alpha = 6.59$; (b). Seven disjoint chaotic attractors for the case FSMRL with $K = 4.5$ and $\alpha = 1.02$. 1000 iterations on each of 20 trajectories: $x_0 = 0$ and $p_0 = 0.0001 + 1.65i$, $0 \leq i < 20$; (c). 20000 iterations on each of two overlapping independent attractors for the FSMC case with $K = 4.5$ and $\alpha = 1.02$. The CBTT has $p_0 = -1.8855$ and the chaotic attractor $p_0 = -2.5135$ ($x_0 = 0$).

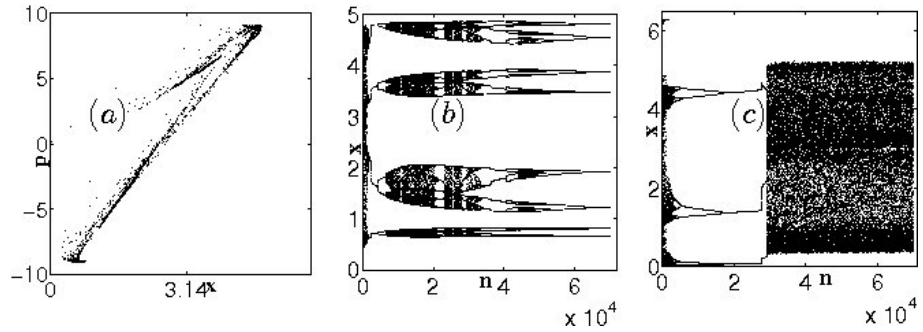


FIGURE 8. The FDSM (in all cases $\Gamma = 5$ and $\Omega = 0$): (a). Phase space for the case $K = 9.1$, $\alpha = 1.2$; (b). 70000 iterations on a single trajectory for the same case as in Figure 8a ($K = 9.1$, $\alpha = 1.2$). A cascade of bifurcations appears from chaos and then converges into a periodic trajectory; (c). 70000 iterations on a single trajectory for the case $K = 10$, $\alpha = 1.2$. A chaotic attractor appears in the FDSM's phase space after a chaotic trajectory through an inverse cascade of bifurcations forms a period $T = 3$ trajectory.

## 4. Conclusion

We studied three different fractional maps which describe nonlinear systems with memory under periodic perturbations (kicks in our case). The types of solutions

which we found in all maps include periodic sinks, attracting slow diverging trajectories, attracting accelerator mode trajectories, chaotic attractors, and cascade of bifurcations type trajectories. New features discovered include attractors which overlap, trajectories which intersect, and CBTTs.

The models with a similar behavior may include periodically kicked media which can be described by FDEs: viscoelastic materials [6] or dielectrics [65]. Experiments can be proposed to observe different kinds of solution, for example CBTTs, in those media.

Nonlinear models with memory which have chaotic and periodic solutions, where cascades of bifurcations considered as a result of a change in a system parameter, are used in population biology and epidemiology [66]. Our calculations show that such behavior can be a consequence of the essential internal properties of the systems with memory and suggest construction of new fractional models of biological systems.

Our computational results are based on the runs over more that $10^5$ periods of perturbations. Due to the integro-differential nature of the fractional derivatives, at present time it is impossible to solve FDEs over more than $10^3$ periods of oscillations. Our results suggest a new way of looking for a particular solutions of the FDEs. For example, we may suggest that CBTTs can be found at the values of system parameters, where in corresponding integer system a period doubling cascade of bifurcations leads to the disappearance of a system of islands.

## References

[1] V. E. Tarasov, *Fractional Dynamics: Application of Fractional Calculus to Dynamics of Particles, Fields and Media.* Springer, HEP, 2011.

[2] V. E. Tarasov, *Theoretical Physics Models with Integro-Differentiation of Fractional Order.* IKI, RCD, 2011 (in Russian).

[3] R. Herrmann, *Fractional Calculus: An Introduction fro Physicists.* World Scientific, Singapore, 2011.

[4] R. Caponetto, G. Dongola, and L. Fortuna, *Fractional Order Systems: Modeling and Control Applications (World Scientific Series on Nonlinear Science Series a).* World Scientific, 2010.

[5] I. Petras, *Fractional-Order Nonlinear Systems.* Springer, 2011.

[6] F. Mainardi, *Fractional Calculus and Waves in Linear Viscoelasticity: An Introduction to Mathematical Models.* Imperial College Press, London, 2010.

[7] A. C. J. Luo and V. Afraimovich (Eds.), *Long-range Interaction, Stochasticity and Fractional Dynamics.* Springer, 2010.

[8] G. M. Zaslavsky, *Hamiltonian Chaos and Fractional Dynamics.* Oxford University Press, Oxford, 2005.

[9] N. Laskin, G. M. Zaslavsky, *Nonlinear fractional dynamics on a lattice with long-range interactions.* Physica A **368** (2006), 38–4.

[10] V. E. Tarasov, G. M. Zaslavsky, *Fractional dynamics of coupled oscillators with long-range interaction.* Chaos **16** (2006), 023110.

[11] N. Korabel, G. M. Zaslavsky, *Transition to chaos in discrete nonlinear Schrödinger equation with long-range interaction.* Physica A **378** (2007), 223–237.

[12] G. M. Zaslavsky, M. Edelman, V. E. Tarasov, *Dynamics of the chain of forced oscillators with long-range interaction: From synchronization to chaos.* Chaos **17** (2007), 043124.

[13] V. E. Tarasov, G. M. Zaslavsky, *Fractional dynamics of systems with long-range space interaction and temporal memory.* Physica A **383** (2007), 291–308.

[14] I. Podlubny, *Fractional Differential Equations.* Academic Press, San Diego, 1999.

[15] R. R. Nigmatullin, *Fractional integral and its physical interpretation.* Theoretical and Mathematical Physics **90** (1992), 242–251.

[16] F. Y. Ren, Z. G. Yu, J. Zhou, A. Le Mehaute, R. R. Nigmatullin, *The relationship between the fractional integral and the fractal structure of a memory set.* Physica A **246** (1997), 419–429.

[17] W. Y. Qiu, J. Lu, *Fractional integrals and fractal structure of memory sets.* Phys. Lett. A **272** (2000), 353–358.

[18] R. R. Nigmatullin, *Fractional kinetic equations and 'universal' decoupling of a memory function in mesoscale region.* Physica A **363** (2006), 282–298.

[19] V. E. Tarasov, G. M. Zaslavsky *Fractional dynamics of systems with long-range space interaction and temporal memory.* Physica A **383** (2007), 291–308.

[20] A. Carpinteri, F. Mainardi, (Eds.), *Fractals and Fractional Calculus in Continuum Mechanics.* Springer, Wien, 1997.

[21] B. N. Lundstrom, A. L. Fairhall, M. Maravall, *Multiple time scale encoding of slowly varying whisker stimulus envelope in cortical and thalamic neurons in vivo.* J. Neuroscience, **30** (2010), 5071–5077.

[22] B. N. Lundstrom, M. H. Higgs, W. J. Spain, A. L. Fairhall, *Fractional differentiation by neocortical pyramidal neurons.* Nature Neuroscience **11** (2008), 1335–1342.

[23] A. A. Kilbas, H. M. Srivastava, J. J. Trujillo, *Theory and Application of Fractional Differential Equations.* Elsevier, Amsterdam, 2006.

[24] A. A. Kilbas, B. Bonilla, J. J. Trujillo, *Nonlinear differential equations of fractional order is space of integrable functions.* Doklady Mathematics **62** (2000), 222–226, Translated from Doklady Akademii Nauk **374** (2000), 445-449. (in Russian).

[25] A.A. Kilbas, B. Bonilla, J.J. Trujillo, *Existence and uniqueness theorems for nonlinear fractional differential equations.* Demonstratio Mathematica **33** (2000), 583–602.

[26] V.E. Tarasov *Differential equations with fractional derivative and universal map with memory.* Journal of Physics A **42** (2009), 465102.

[27] A. Wineman, *Nonlinear viscoelastic membranes.* Computers and Mathematics with Applications **53** (2007), 168–181.

[28] A. Wineman, *Nonlinear Viscoelastic Solids - A Review.* Mathematics and Mechanics of Solids **14** (2009), 300–366

[29] F. Hoppensteadt, *Mathematical Theories of Populations: Demographics, Genetics, and Epidemics.* SIAM, Philadelphia, 1975.

[30] F. Brauer, C. Castillo-Chavez, *Mathematical Models in Population Biology and Epidemiology.* Springer, New York, 2001.

[31] V. Gafiychuk, B. Datsko, *Mathematical modeling of different types of instabilities in time fractional reaction-diffusion systems.* Computers and Mathematics with Applications **59** (2010), 1001–1007.

[32] V. Gafiychuk, B. Datsko, V. Meleshko, D. Blackmore, *Analysis of the solutions of coupled nonlinear fractional reaction-diffusion equations.* Chaos, Solitons & Fractals **41** (2009), 1095–1104.

[33] V. Gafiychuk, B. Datsko, *Stability analysis and limit cycle in fractional system with Brusselator nonlinearities.* Phys. Let. A **372** (2008), 4902–4904.

[34] V. Gafiychuk, B. Datsko, V. Meleshko, *Analysis of fractional order Bonhoeffer-van der Pol oscillator.* Physica A **387** (2008), 418–424.

[35] G. M. Zaslavsky, A. A. Stanislavsky, M. Edelman, *Chaotic and pseudochaotic attractors of perturbed fractional oscillator.* Chaos **16** (2006), 013102.

[36] M. S. Tavazoei, M. Haeri, *Chaotic attractors in incommensurate fractional order systems.* Physica D **237** (2008), 2628–2637.

[37] V. E. Tarasov, G. M. Zaslavsky, *Fractional equations of kicked systems and discrete maps.* J. Phys. A **41** (2008), 435101.

[38] M. Edelman, V. E. Tarasov, *Fractional standard map.* Phys. Let. A **374** (2009), 279–285.

[39] V. E. Tarasov, M. Edelman, *Fractional dissipative standard map.* Chaos **20** (2010), 023127.

[40] V. E. Tarasov, *Discrete map with memory from fractional differential equation of arbitrary positive order.* Journal of Mathematical Physics. **50** (2009), 122703.

[41] B. V. Chirikov, *A universal instability of many dimensional oscillator systems.* Phys. Rep. **52** (1979), 263–379.

[42] G. M. Zaslavsky, *The simplest case of a strange attractor.* Phys. Lett. A **69** (1978), 145–147.

[43] G.M. Zaslavsky, Kh.-R. Ya. Rachko, *Singularities of transition to a turbulent motion.* Sov. Phys. JETP **49** (1979), 1039–1044.

[44] A. J. Lichtenberg, M. A. Lieberman, *Regular and Chaotic Dynamics.* Springer, Berlin, 1992.

[45] G. M. Zaslavsky, *Hamiltonian Chaos and Fractional Dynamics.* Oxford University Press, Oxford, 2005.

[46] E. Ott, *Strange Attractors and Chaotic Motions of Dynamical Systems.* Rev. Mod. Phys. **53** (1981), 655–671.

[47] V. Afraimovich, Sze-Bi Hsu, *Lectures on Chaotic Dynamical Systems.* Amer. Math. Society. International Press, Providence, 2002.

[48] P. Grassberger and I. Procaccia, *Measuring the strangeness of strange attractors.* Physica D **9** (1983), 189-208.

[49] D. A. Russel, J. D. Hanson, and E. Ott, *Dimension of strange attractors.* PRL **45** (1980), 1175–1178.

[50] F. Haake, *Quantum Signatures of Chaos.* Springer, Berlin, 2000.

[51] G.M. Zaslavsky, M. Edelman, *Superdiffusion in the Dissipative Standard Map.* Chaos **18** (2008), 033116.

[52] Q. Wang and L.-S. Young, *From invariant curves to strange attractors.* Commun. in Math. Phys. **bf 225** (2002), 275–304.

[53] Q. Wang and L.-S. Young, *Strange attractors in periodically-kicked limit cycles and Hopf bifurcations.* Commun. in Math. Phys. **240** (2003), 509–529.

[54] M. Edelman, *Fractional Standard Map: Riemann-Liouville vs. Caputo.* Commun. Nonlin. Sci. Numer. Simul, **16** (2011), 4573-4580.

[55] A. Fulinski, A. S. Kleczkowski, *Nonlinear maps with memory.* Physica Scripta **35** (1987), 119–122.

[56] E. Fick, M. Fick, G. Hausmann, *Logistic equation with memory.* Phys. Rev. A **44** (1991), 2469–2473.

[57] K. Hartwich, E. Fick, *Hopf bifurcations in the logistic map with oscillating memory* Phys. Lett. A **177** (1993), 305–310.

[58] M. Giona, *Dynamics and relaxation properties of complex systems with memory.* Nonlinearity **4** (1991), 911–925.

[59] J. A. C. Gallas, *Simulating memory effects with discrete dynamical systems.* Physica A **195** (1993), 417–430; *Erratum.* Physica A **198** (1993), 339–339.

[60] A. A. Stanislavsky, *Long-term memory contribution as applied to the motion of discrete dynamical system.* Chaos **16** (2006), 043105.

[61] G. Schmidt, *Stochasticity and fixed-point transitions.* Phys. Rev. A **22** (1980), 2849–2854.

[62] Y. Li, Y.Q. Chen, I. Podlubny, *Stability of fractional-order nonlinear dynamic systems: Lyapunov direct method and generalized Mittag-Leffler stability.* Comput. Math. Appl. **59** (2010), 1810–1821.

[63] M. Edelman, *Cascade of bifurcation type trajectories in fractional dynamical systems* submitted to Chaos.

[64] G.M. Zaslavsky, M. Edelman, B.A. Niyazov, *Self-Similarity, renormalization, and phase space nonuniformity of Hamiltonian chaotic dynamics.* Chaos **7** (1997), 159-181.

[65] V. E. Tarasov, *Universal electromagnetic waves in dielectrics.* J Phys.: Condens. Matter **20** (2008), 175223.

[66] F. Hoppensteadt, *A nonlinear renewal equation with periodic and chaotic solutions.* SIAM-AMS Proc. **10** (1976), 51–60.

**Acknowledgment**

The authors express their gratitude to the administration of the Stern College, Courant Institute, and DOE Grant DE-FG0286ER53223 for the financial support.

Mark Edelman
Stern College for Women at Yeshiva University
245 Lexington Ave.
New York, NY 10016
USA
e-mail: edelman@cims.nyu.edu

Laura Anna Taieb
Stern College for Women at Yeshiva University
245 Lexington Ave.
New York, NY 10016
USA
e-mail: taieb@yu.edu